Journal of Materials Chemistry C

Accepted Manuscript

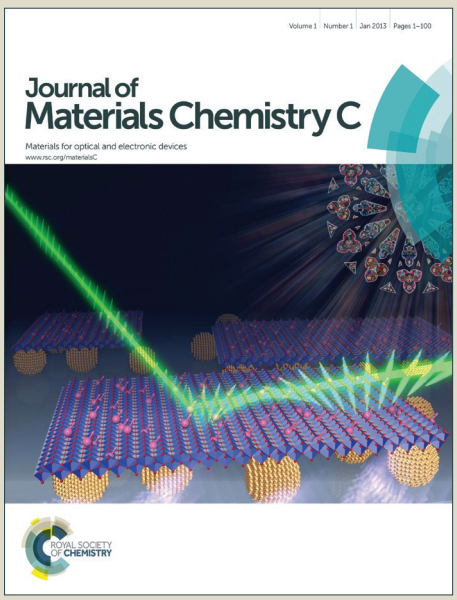

ROYAL SOCIETY OF CHEMISTRY

www.rsc.org/materialsC

Journal Name

RSCPublishing

ARTICLE

Design of rewritable and read-only non-volatile optical memory elements using photochromic spiropyran-based salts as light-sensitive materials

Cite this: DOI: 10.1039/x0xx00000x

Received 00thMarch 2014,
Accepted 00th January 2012

DOI: 10.1039/x0xx00000x

www.rsc.org/

L. A. Frolova,[a] A. A. Rezvanova,[a] B. S. Lukyanov,[b] N. A. Sanina,[a] P. A. Troshin[a*] and S. M. Aldoshin[a]

Here we applied photochromic spiropyran-based salts **SP1** and **SP2** as light-sensitive components of the OFET-based non-volatile optical memory elements. Electrooptical programming by applying simultaneously light bias and gate (programming) voltage allowed us to demonstrate wide memory windows, high programming speeds (programming time of 0.5-20 ms), and good retention characteristics of the devices. It is remarkable that a minor difference in the molecular structures of the used spiropyran-based salts (hydrogen atom in the structure of **SP1** is replaced with NO_2 group in **SP2**) altered completely the behavior of the devices. Thus, the OFETs comprising interlayers of the spiropyran-based salt **SP1** showed a reversible photoelectrical switching which is characteristic for flash memory elements with good write-read-erase cycling stability. On the contrary, the devices based on the spiropyran-based salt **SP2** demonstrated irreversible switching and operated as read-only memory (ROM). Both types of devices revealed the formation of multiple distinct electrical states thus resembling the behavior of multibit memory elements capable of high-density information storage.

Introduction

Recent flow of publications reflects a rising interest of the research community to the application of different types of photochromic compounds in the design of advanced organic electronic devices.[1-4] Organic photochromes undergo facile photoinduced isomerization between two quasi stableforms which differ significantly by their frontier energy levels, electrical conductivity, dipole moment, dielectric constant and etc.[5] In particular, a bistable nature of the most common photochromic compounds inspired their application in the design of memory devices.[1]

Many researchers investigated diode-type memory cell configuration comprising photochromic materials in the active layer sandwiched between two electrodes.[6] Light-induced isomerization of the photochromic component results in the formation of bipolar traps affecting transport of charges between the electrodes of the device.[7] Alternatively, photochromic molecules can be disposed at the interface between the semiconductor layer and one of the electrodes thus governing the charge injection in the diode device. This approach has been used for an elegant demonstration of large-area OLEDs with optical memory capabilities.[8]

In spite of a considerable progress in the field of the diode-type memory devices, the achieved photoswitching effects were not very high (with a few notable exceptions[4,9]) thus challenging their practical implementation. This might be one of the reasons why transistor-type memory elements comprising photochromic materials have attracted much attention of the researchers recently.[1] While comparing the characteristics of the transistor-based memory elements a few important parameters should be considered. First of all, it is a switching coefficient defined as $k_{sw}=I_{DS}$(state 1)/I_{DS}(state 2) which shows how strong is the hysteresis in the electrical characteristics of the transistor or how wide is the memory window. The device operating voltages, programming speed and long-term stability of distinct electrical states (retention characteristics) are also crucially important.

The most explored device architecture includes a photochromic compound mixed with a semiconductor material in the structure of organic field-effect transistors (OFETs).[10] However, such modification results in a charge trapping in the semiconductor layer which affects considerably all electrical characteristics of the OFETs. The best devices of this type showed switching coefficients k_{sw} of 5-18 which are comparable to the characteristics achieved in the diode-type memory devices.[6] Alternatively, thin layers (or even monolayers) of photochromic molecules are inserted under the source and/or drain electrodes in order to control the charge injection in OFETs.[11]However, the obtained parameters (k_{sw}~2-3) were inferior compared to the results obtained by introducing photochromic material as "dopant" to the semiconductor layer.[12]

It is known that the highest density of the charge carriers in operating OFET flows in a few molecular layers of semiconductor adjacent to dielectric.[13] Therefore, the photoisomerization of a photochromic compound at the dielectric/semiconductor interface changes significantly electrical characteristics of the conducting channel (density of traps/carriers, electrical permittivity, capacitance) and the

device itself thus providing the required photoswitching effect.[14-15] This approach has been pursued by several research groups, however, the achieved switching coefficients were also not very high (k_{sw}=0.3-10).[12-16]

Analyzing previous reports on the OFET-based optical memories based on photochromic materials one can notice their modest switching coefficients (Table S1, Electronic Supplementary Information, ESI). These devices typically operate at high voltages (30-100 V), while their programming is slow and requires tens of seconds or even minutes. To make this type of memory more interesting for practical applications one has to improve significantly the main device characteristics.

We have reported very recently memory elements based on a commercial photochromic spirooxazine which showed reasonably operating voltages (<5 V) and high switching coefficients of ~10^3.[17] Unfortunately, the programming speeds were still low mainly due to fundamental limitations of the used material and the device architecture.

In the present work we continued our work on exploring different types of photochromic compounds as light-sensitive materials for designing OFET-based optical memories. It has been shown that the rationally designed spiropyran-based salts **SP1** and **SP2** (see Scheme 1 below) can be used successfully to produce memory devices with advanced electrical characteristics and high programming speeds.

Results and discussion

The compounds **SP1** and **SP2** reported in this work were synthesized according to the Scheme 1. The precursor spiropyran **1** comprising quinoline unit in its molecular framework was treated with the corresponding benzyl halides **2a** or **2b** in anhydrous acetone in the presence of a large excess of NaI. Slow crystallization produced pure compounds **SP1** and **SP2** with acceptable yields (see Experimental).

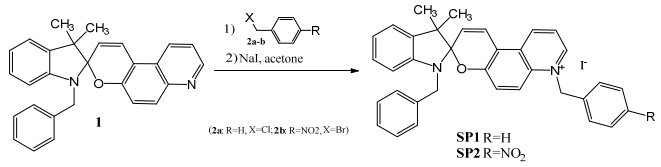

Scheme 1 Synthesis of the spiropyran-based salts **SP1** and **SP2**

It is known that the thermodynamically stable closed forms of the spiropyran-based salts undergo reversible photoisomerization in solution to the quasi-stable open zwitterionic isomers under illumination in solution with UV or violet light. Back transition occurs when the system is illuminated with a visible light or at elevated temperatures (Scheme 2). However, the photochromic behavior of the spiropyran-based salts is strongly inhibited in a solid state.[5] Therefore, this makes challenging their application for light-triggering of the thin film electronic devices.

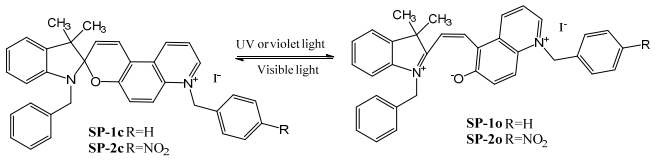

Scheme 2. Reversible photoisomerization of the spiropyran-based salts

We investigated optical properties of the spin-coated films of **SP1** and **SP2** (thickness ca. 150 nm) before and after illumination with a violet diode laser (λ=405 nm, light intensity ~60 mW/cm^2). The spectra of the films revealed that both compounds have intense absorption bands at the laser wavelength (Fig. 1). However, **SP1** showed much stronger response to the violet light as compared to the **SP2**. Indeed, the intensity of the 550-650 nm absorption band noticeably increased in the spectrum of the **SP1** film after illumination thus proving that violet light leads to the accumulation of the zwitter-ionic form of this compound. On the contrary, the absorption spectrum of the **SP2** film was just slightly affected by illumination under the same conditions. These results imply that just a minor difference in the molecular structures of the spiropyran-based salts (e.g. replacing H with NO_2) can affect significantly their photochromic behavior in thin films.

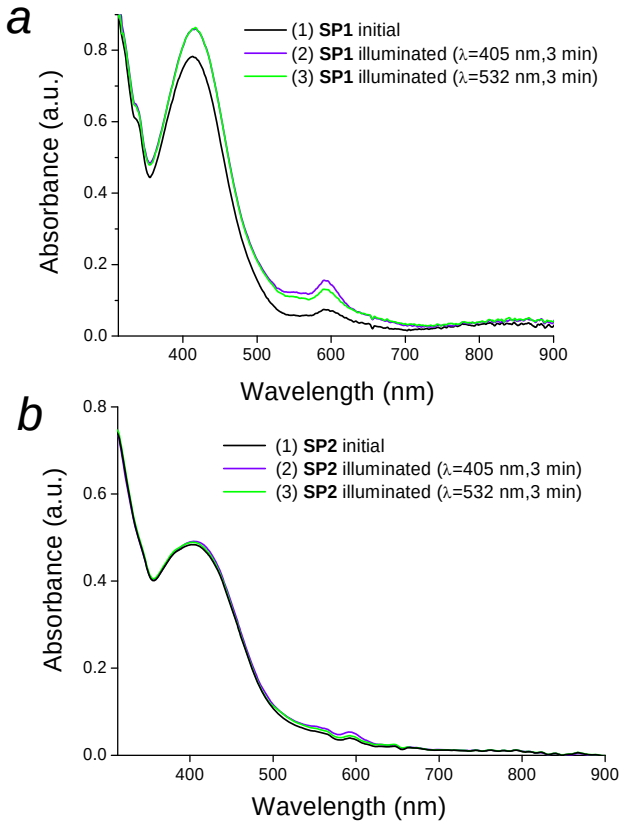

Figure 1 The absorption spectra of thin films of the spiropyran-based salts SP1 (a) and SP2 (b) in a pristine (as coated) state (1), after illumination with a violet light for 3 min. (2) and then after subsequent illumination with a green light for additional 3 min. (3)

It is also notable that the illumination of the **SP1** and **SP2** films with a green diode laser (λ=532 nm, light intensity ~80 mW/cm^2) leads to a very weak decrease in the intensity of the 550-650 nm bands (Fig. 1). This strongly suggests that backward isomerization of the zwitter-ionic forms of both spiropyran-based salts is strongly inhibited in thin films. Therefore, a simple optical programming (using pulses of violet and green laser) cannot provide significant photoswitching effects in diodes or transistors comprising thin films of the spiropyran-based salts **SP1** or **SP2**.

In the present work both spiropyran-based salts were investigated as light–sensitive components in the structure of the photoswitchable OFETs. The architecture of the devices is shown schematically in Fig. 2. To construct such devices, aluminum gate electrodes were initially subjected to anodic oxidation in order to grow thin AlO_x dielectric layer. Afterwards, the photoactive spiropyran-based salt layer was spin-coated from a solution in chlorobenzene. We note here that investigated spiropyrans do not show semiconductor properties and, therefore, the fabricated OFETs comprise hybrid AlO_x/spiropyran dielectrics. Fullerene C_{60} applied as n-type semiconductor in this work was deposited by sublimation in vacuum. Finally, silver source and drain electrodes were evaporated through a shadow mask forming a transistor channel with W=2 mm and L=60 μm.

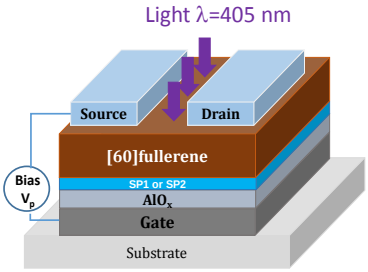

Figure 2. A schematic layout of the investigated OFET-based memory elements comprising spiropyran-based salts SP1 or SP2 as light-sensitive components.

While programming the memory elements, we applied an electrical bias between the source and gate electrodes of the transistor (programming voltage V_p) and illuminated the channel of the device with a violet light (λ=405 nm, light intensity ~60 mW/cm^2) as it is shown schematically in Fig. 2. The length of the single laser pulse was changed between 0.5 ms and 100-200 ms in a controlled fashion in order to reveal the actual operation speed of the memory elements. The transfer characteristics of the devices were measured after each programming step.

Figure 3 shows that both types of devices comprising spiropyran-based salts **SP1** and **SP2** show increase in the threshold voltage under programming with positive V_p potentials in combination with light (λ=405 nm). Switching of the devices occurs with a remarkably high speed: the I_{DS} currents monitored at the constant V_{GS}= 2.4 V potential are decreased by more than one order of magnitude within 0.5-2.0 ms. Increase in the programming time up to 15-17 ms allows one to achieve impressive switching coefficients $k_{sw}>10^4$. Programming with a negative V_p bias and light (λ=405 nm) for 50 ms allows one to accomplish a backward transition of the devices based on **SP1** (Fig. 3c, Fig. S1a). On the contrary, devices comprising **SP2** could not be reversed by applying negative programming voltages (Fig. 3d, Fig. S1b). Therefore, the discrete electrical states induced in the **SP2**-based devices under the positive V_p bias have irreversible nature.

Considering potential applications of the designed devices, one can notice that OFETs comprising **SP1** demonstrate flash type memory operation which means that information can be written, read and erased for many times. In the case of the **SP2**-based devices, the information can be written just once and read for many times. This corresponds to the read-only type of memory (ROM). Both flash memory and ROM memory can find useful applications in the design of a variety of organic electronics products.

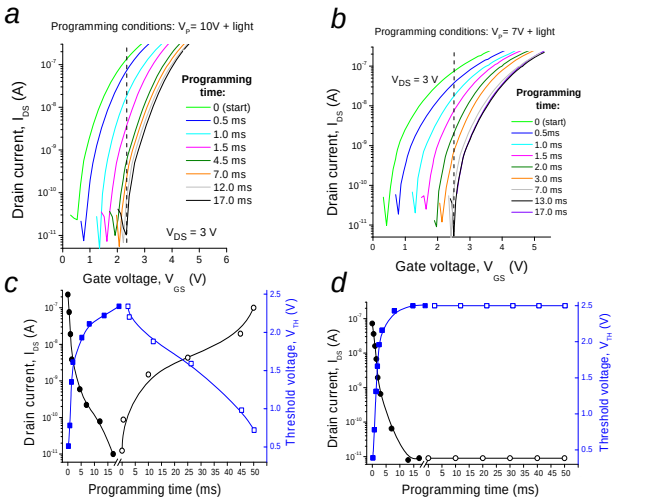

Figure 3. Evolution of the transfer characteristics of the devices comprising **SP1** (a) and **SP2** (b) under positive applied voltage (V_p=10 V for **SP1** and V_p=7 V for **SP2**) and violet light (λ=405 nm) as a function of the programming time. Evolution of the OFET drain currents (circles) and threshold voltages (squares) while programming the devices comprising **SP1** (c) and **SP2** (d) first with positive V_p (closed symbols) and then with negative V_p (open symbols) potentials.

The revealed striking difference in the behavior of the photoswitchable OFETs comprising the spiropyran-based salts **SP1** and **SP2** should be related to the peculiarities of their molecular structures. Most likely, the presence of the nitro group in the **SP2** molecule is responsible for the observed irreversible photoswitching effect in OFETs.

The device behavior correlates to some extent with the optical properties of the bilayer spiropyran/C_{60} films modeling the photoactive dielectric/semiconductor interface. Indeed, **SP2**/C_{60} films were almost insensitive to the violet light: continuous illumination within 3 min. induced just negligibly small spectral changes (Fig. S2b, ESI). On the contrary, the **SP1**/C_{60} bilayer films studied under the same conditions showed a strong increase in the absorbance at 550-650 nm thus revealing the accumulation of the photonduced zwitter-ionic isomer.

In our previous study of the photoswitchable OFETs based on the spirooxazine/C_{60} junctions we have shown that the formation of the ground-state charge transfer complexes at the interface between the C_{60} and the photochromic material plays an important role in the device operation.[17] One can assume that photo-OFETs based on the **SP1**/C_{60} bilayer system work *via* a very similar mechanism. However, the presence of the strong electron withdrawing nitro group in the molecule of **SP2** reduces dramatically its electron donating ability and thus inhibits the formation of the charge transfer complexes with C_{60}. Blocking this charge transfer complex pathway alters significantly the photoswitching behavior of the OFETs based on the bilayer **SP2**/C_{60} films.

It has been shown that using different programming voltages can induce multiple and highly reproducible discrete electrical states in the OFETs comprising **SP1** or **SP2** as light-sensitive materials. It is seen from the Fig. 4 that programming OFETs in the initial state with the light under negative V_p potentials does not produce any significant changes. However, the application of the positive V_p and light results in a controllable shift of the device threshold voltage (V_{TH}) from ca. 0 V to 4.7 V (**SP1**) and from ca. 2.0 V to 6.5 V (**SP2**). The devices comprising **SP1** undergo a backward transition (V_{TH} shifts from 4.7 V to ~0 V) under programming with a negative V_p bias (-10 V) and light.

It should be emphasized that only simultaneous action of the electrical bias and light induces the observed programming effects. The application of the electrical bias or light alone at the programming step induces just negligible changes in the transistor threshold voltage V_{TH} (black lines in Fig. 4c-d).

The V_{TH}-V_p dependences shown in Fig. 4 illustrate a sharp difference in the behavior of the OFETs comprising different spiropyran-based salts. In the case of **SP1**-based devices just a reasonable hysteresis was observed (Fig. 4c) thus suggesting that this system is fully reversible. On the contrary, OFETs comprising **SP2** revealed a huge hysteresis due to their complete irreversibility (Fig. 4d).

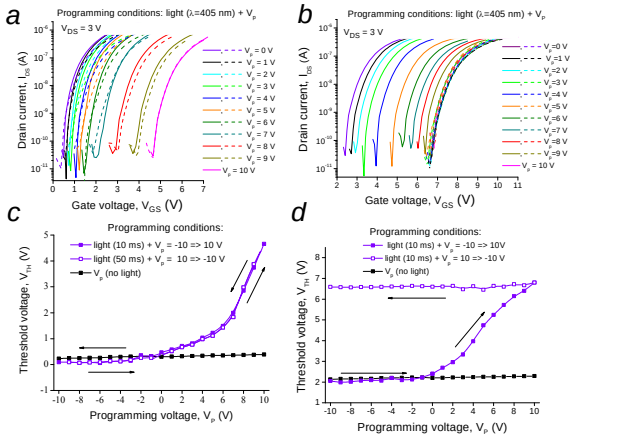

Figure 4. Transfer characteristics of the OFETs comprising **SP1** (a) and **SP2** (b) switched by applying different V_p voltages (going from 0 V to 10 V (solid lines) and back (dashed lines)) and violet light (λ=405 nm) for 20 ms. Evolution of the OFET threshold voltage as a function of the programming voltage for the systems based on **SP1** (c) and **SP2** (d).

Considering the potential multibit memory applications of the designed devices, special attention has to be paid to their stability and reliability, as well as to the achievable switching coefficients. In order to check the device stability, evolution of the transfer characteristics of OFETs in time was investigated (Fig. 5). It has been shown that both high current state (state "1") and low current state (state "2") are very stable over a considerable period of time (~3×10^6 s, ca. 1 month). At the same time, both types of devices demonstrated impressive current ratios between these two states approaching 1.36×10^4 in the case of **SP1** (V_{GS}=1.78 V) and 1.4×10^4 in the case of **SP2** (V_{GS}=4.17 V).

The devices based on **SP2** cannot be switched reversibly between the states "1" and "2". Therefore, initially we followed the stability of the state "1" (with a lower V_{TH}), then performed programming with V_p=7 V and light for 20 ms and studied the stability of the high current state "2".

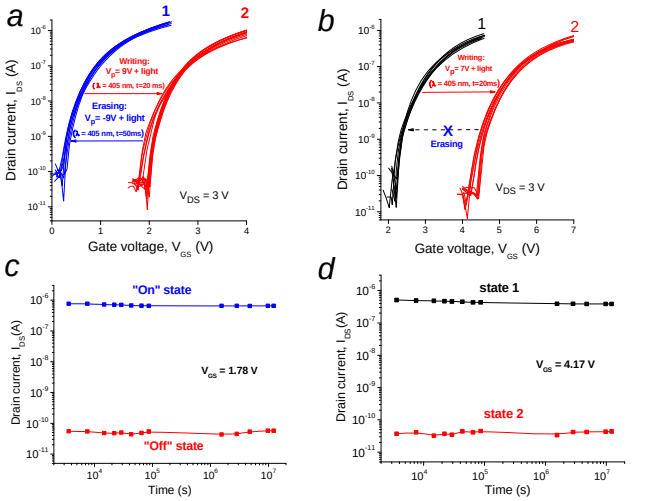

Figure 5. Periodically measured transfer characteristics of the OFETs (a, b) and corresponding drain currents plotted as a function of time (c, d) illustrating a superior stability of two distinct electrical states of OFETs comprising **SP1** (a, b) or **SP2** (c, d).

The OFETs based on **SP1** can be switched many times with a high accuracy between any two arbitrary selected states. Figure 6 shows twenty manually recorded "write-read-erase" cycles which demonstrate appreciable reproducibility and cycling stability of these devices.

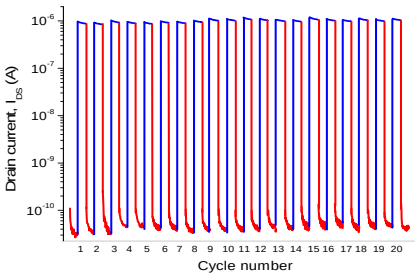

Figure 6. Write-read-erase cycling behavior of the devices comprising **SP1** as a light-sensitive material

Retention characteristics presented in Fig. 5c also prove the capability of applying the designed photoswitchable OFETs as non-volatile flash memory elements.

Conclusion

In conclusion, we have demonstrated that the photochromic spiropyran-based salts can be successfully utilized as light-sensitive materials in the design of photoswitchable OFETs demonstrating impressive electrical characteristics such as wide memory windows, low operation voltages, switching coefficients exceeding 10^4, high switching speeds leading to the short programming times ranging from 0.5-2.0 ms to 20 ms.

It has been revealed that relatively small change in the molecular structure of the photochromic spiropyran-based salt can alter completely the device behavior. Thus, the OFETs based on the pristine (H-substituted) spiropyran-based salt **SP1** operated as non-volatile flash memory elements with good electrical characteristics and excellent write-read-erase cycling reproducibility and stability. On the contrary, the devices comprising NO_2-substituted spiropyran-based salt **SP2** showed irreversible photoelectrical switching behavior thus resembling the operation of the ROM memory elements.

The observed remarkable effect of the material structure on the device performance can be applied in the future for tuning the electrical parameters of the OFETs and designing multibit optical memory elements with advanced operational characteristics, good stability and reliability.

Experimental

Synthesis and spectral characteristics of epy spiropyran-based salts

Spiro-1-benzyl-3,3-dimethylindolin-2,3'-[3H]pyrano[3,2-f] quinoline] (compound **1**, Scheme 1). 1.1 ml (13 mmol) of piperidine was dropwise added to a boiling mixture of 3.08 g (8.1 mmol) of 1-benzyl-2,3,3-trimetilindoline iodide and 1.90 g (11 mmol) of 6-hydroxyquinoline-5-aldehyde in 15 ml of isopropanol. The reaction mixture was heated 15 minutes at reflux and then kept overnight at room temperature. The precipitate was isolated by filtration and purified by recrystallization from n-hexane. Yield: 39%, mp 100-101^{0}C.

Chemical analysis for **$C_{28}H_{24}N_2O$.** Found (%):C, 83.21; H, 5.93; N, 6.90; Anal. Calcd. (%):C, 83.17; H, 5.94; N, 7.72.

FTIR (cm^{-1}): ν_{C-O} 927; ν_{Cap-O} 1073; ν_{C-N} 1253; $\nu_{C=N}$ 1476; $\nu_{C=C}$ 1576, 1600, 1640.

^{1}H NMR: δ, ppm, (*J*, Hz): 1.32 (H, s, gem. –CH_3); 1.4 (3H, s, gem. –CH_3); 4.37 (2H, d.d, *J* = 16.42, –CH_2–Ar); 5.9 (1H, d, *J* = 10.4, H-2′); 6.3 (1H, d, *J* = 7.6, H-6′); 6.86 (1H, d, *J* = 7.6, H-5′); 7.02-7.14 (8H, m, –ArH); 7.38 (1H, d, *J* = 8.2, H-10′); 7.45 (1H, d, *J* = 10.4, H-1′); 7.89 (1H, d, *J* = 9.16, H-4); 8.29 (1H, d, *J* = 8.21, H-7); 8.75 (1H, d.d, *J* = 4.1, H-8′).

Spiro[1,7'-dibenzyl-3,3-dimethylindolin-2,3'-[3*H*]-pyran [3,2-*f*]quinoliny] iodide (compound **SP1**, Scheme 1). A mixture of 0.25 g (0.62 mmol) of **1**, 0.074 g (0.584 mmol) of benzyl chloride, twenty-fold excess of NaI and 15 ml of absolute acetone was introduced into a round-bottom flask equipped with a reflux condenser and a calcium chloride tube. The reaction mixture was heated at reflux for 3.5 hours and then it was stored at room temperature for two days until a complete precipitation of the product and sodium chloride was observed. The precipitate was isolated by filtration and the target compound **SP1** was extracted with warm absolute acetone. Yield: 55%, mp 176-179^{0}C.

Chemical analysis for **$C_{35}H_{31}N_2OI$.** Found (%):C, 67.47; H, 4.95; N, 4.54; Anal. Calcd. (%):C, 67.52; H, 4.98; N, 4.50.

FTIR (cm^{-1}): ν_{C-O} 916; ν_{Cap-O} 1046; ν_{C-N} 1287; $\nu_{C=N}$ 1456; $\nu_{C=C}$ 1577, 1600, 1638.

^{1}H NMR: δ, ppm, (*J*, Hz): 1.32 (6H, s, gem. (–CH_3)$_2$); 4.32 (2H, d.d, *J* = 16.4, $N_{(1)}$–CH_2–Ar); 6.10 (1H, d, *J* = 10.4, H-2′); 6.35 (1H, d, *J* = 7.6, H-4); 6.46 (2H, s, $N_{(7')}$–CH_2–Ar); 6.88-7.33 (13H, m, ArH); 7.41 (1H, d, *J* = 9.7, H-6′); 7.64 (1H, d, *J* = 10.4, H-1′); 8.10 (1H, d, *J* = 9.7, H-5′); 8.19 (1H, t, J_1 = 5.5 (H-8′), J_2 = 8.5 (H-10′), H9′); 9.33 (1H, d, *J* = 8.5, H-10′); 10.13 (1H, d, *J* = 5.5, H-8′).

Spiro[1-benzyl-3,3-dimethyl-7′-*p*-nitrobenzylindolin-2,3'-[3*H*]-pyran [3,2-*f*]quinoliny] iodide (compound **SP2**, Scheme 1). A mixture of 0.768 g (1.889 mmol) of **1,** 0.431 g (1.994 mmol) of p-nitrobenzyl bromide, twenty-fold excess of NaI and 50 ml of absolute acetone was introduced into a round-bottom flask equipped with a reflux condenser and a calcium chloride tube. The reaction mixture was heated at reflux for 3.5 hours and then it was stored at room temperature for two days until a complete precipitation of the product was observed. The formed precipitate of **SP2** and NaBr was collected by filtration. The target **SP2** was extracted with chloroform, concentrated in vacuum and the resulting oily residue was triturated in acetone. Yield: 60%, mp 141-144^{0}C.

Chemical analysis for **$C_{35}H_{30}N_3O_3I$**. Found (%): C, 62.97; H, 4.47; N, 6.31; Anal. Calcd. (%):C, 62.97; H, 4.53; N, 6.29.

IR spectra for 1 (cm^{-1}): ν_{C-O} 919; ν_{Cap-O} 1047; ν_{C-N} 1280; $\nu_{C=N}$ 1460; $\nu_{C=C}$ 1573, 1600, 1633.

^{1}H NMR: δ, m. d., (*J*, Hz): 1.31 (6H, s, gem. $(CH_3)_2$); 4.32 (2H, d.d, *J* = 16.5, –CH_2–Ar); 6.13 (1H, d, *J* = 10.5, H-2′); 6.33-8.13 (16H, m, ArH); 6.91 (2H, s, –CH_2–ArNO_2); 7.46 (1H, d, *J* = 10.5, H-1′); 9.23 (1H, d, *J* = 8.8, H-5′); 10.32 (1H, d, *J* = 5.3, H-8′).

Fabrication and characterization of the memory elements

The photoswitchable OFETs and memory devices were fabricated on glass substrates. The glass slides were cleaned by sonication in a base piranha solution (a mixture of hydrogen peroxide and ammonia, both obtained from ChimMed, Russia), rinsed with deionized water and dried in an oven at 60^{o}C for 30 min. UV plasma treatment (150 W) was applied additionally for 10 min. Afterwards, aluminum gate electrodes with a thickness of 200 nm were deposited by thermal evaporation in vacuum (2×10^{-6} mbar) through a shadow mask. Afterwards, AlO_x (~10 nm) was grown by anodic oxidation of aluminum gate electrodes in 0.01 mol citric acid (Acros Organics) at the constant potential of 12 V. Afterwards, the samples were rinsed with deionized water and dried in a vacuum oven at 60^{o}C for 30

min. A toluene solution of the spiropyran-based salt (**SP1** or **SP2**, 10 mg·mL^{-1}) was spin coated at 750 rpm onto the aluminum oxide layer inside a nitrogen glove box (MBraun Unilab) producing the uniform films with the thickness of 15-20 nm. Then the samples were transferred to a vacuum chamber (also integrated inside the glove box) and [60]fullerene was thermally deposited with a rate of 0.3–0.4 nm s^{-1} at 320°C under vacuum (2×10^{-6} mbar) to form a 100 nm thick semiconductor layer. The devices were finalized by evaporating 100 nm thick silver source and drain electrodes through a shadow mask. The channel length (L) and width (W) were 60 and 2000 μm, respectively.

The electrical characterization of the devices was performed using double-channel Keithley 2612A instrument under inert atmosphere inside glove box. A diode laser with a power of ~ 20 mW (corresponds to the light intensity ~60 mW/cm^2) and a sharp maximum at 405 nm modulated with Advantest R6240A was used for programming the memory elements.

Acknowledgements

This work was supported by the Russian Foundation for Basic Research (grants 15-03-06175 and 13-03-00631) and the Research Program of the Presidium of the Russian Academy of Sciences (No. 35).

Notes and references

[a] Institute for Problems of Chemical Physics of Russian Academy of Sciences (IPCP RAS), Semenov Prospect 1, Chernogolovka, 142432, Russia. Fax: +7 496515-5420; Tel: +7 496522 1418; E-mail: troshin2003@inbox.ru

[b] Southern Federal University, Rostov-on-Don, Bolshaya Sadovaya Str. 105/42, 344006, Russia

Electronic Supplementary Information (ESI) available: a selection of the literature data on the OFET-based optical memory elements comprising photochromic compounds as light-sensitive materials, transfer characteristics of the OFETs programmed under negative V_p voltages, absorption spectra of the bilayer spiropyran/C_{60} films before and after illumination with a violet light.See DOI: 10.1039/b000000x/

References

1 E. Orgiu, P. Samorì, *Adv. Mater*. 2014, **26**, 1827.

2 T. Tsujioka, M. Irie, *J. Photochem. Photobiol. C* 2010, **11**, 1.

3 J. J. Zhang, Q. Zou, H. Tian, *Adv. Mater.* 2013, **25**, 378.

4 R. C. Shallcross, P. Zacharias, A. Koehnen, P. O. Koerner, E. Maibach, K. Meerholz, *Adv. Mater.* 2013, **25**, 469.

5 V. I. Minkin, Chem. Rev. 2004, 104, 2751; M. Irie, T. Fukaminato, K. Matsuda, S. Kobatake, *Chem. Rev.*, 2014, **114**, 12174

6 T. Tsujioka, H. Kondo, *Appl. Phys. Lett*. 2003, **83**, 937; T. Tsujioka, K. Masuda, *Appl. Phys. Lett*. 2003, **83**, 4978; T. Tsujioka, M. Shimizu, E. Ishihara, *Appl. Phys. Lett*. 2005, **87**, 213506; P. Andersson, N. D. Robinson, M. Berggren, *Synth. Met*. 2005, **150**, 217; M. Weiter, M. Vala, O. Zmeskal, S. Nespurek, P. Toman, *Macromol. Symp*. 2007, **247**, 318.

7 S. Nespurek, J. Sworakowski, C. Combellas, G. Wang, M. Weiter, *Appl. Surf. Sci.* 2004, **234**, 395; P. Andersson, N. D. Robinson, M. Berggren, *Adv. Mater*. 2005, **17**, 1798.

8 P. Zacharias, M. C. Gather, A. Koehnen, N. Rehmann, K. Meerholz, *Angew. Chem. Int. Ed.* 2009, **48**, 4038.

9 R. C. Shallcross, P. O. Körner, E. Maibach, A. Köhnenand K. Meerholz, *Adv. Mater*., 2013, **25**, 4807

10 Y. R. Li, H. T. Zhang, C. M. Qi, X. F. Guo, *J. Mater. Chem*. 2012, **22**, 4261; C. Raimondo, N. Crivillers, F. Reinders, F. Sander, M. Mayor, P. Samorì, *Proc. Natl. Acad. Sci. U.S.A.* 2012, **109**, 12375; Y. Ishiguro, R. Hayakawa, T. Chikyow, Y. Wakayama, *J. Mater. Chem. C* 2013, **1**, 3012; M. E. Gemayel, K. Börjesson, M. Herder, D. T. Duong, J. A. Hutchison, C. Ruzié, G. Schweicher, A. Salleo, Y. Geerts, S. Hecht, E. Orgiu, P. Samorì, *Nature Comm*., 2015, **6**, 6330; K. Börjesson, M. Herder, L. Grubert, D. T. Duong, A. Salleo, S. Hecht, E. Orgiu, P. Samorì, *J. Mater. Chem. C*, 2015, **3**, 4156.

11 Q. Shen, Y. Cao, S. Liu, M. L. Steigerwald, X. Guo. *J. Phys. Chem. C.* 2009, **113**, 10807

12 N. Crivillers, E. Orgiu, F. Reinders, M. Mayor, P. Samorì, Adv. Mater. 2011, 23, 1447

13 R. Ruiz, A. Papadimitratos, A. C. Mayer, G. G. Malliaras, *Adv. Mater.* 2005, **17**, 1795.

14 P. Lutsyk, K. Janus, J. Sworakowski, G. Generali, R. Capelli, M. Muccini, *J. Phys. Chem. C* 2011, **115**, 3106.

15 Q. A. Shen, L. J. Wang, S. Liu, Y. Cao, L. Gan, X. F. Guo, M. L. Steigerwald, Z. G. Shuai, Z. F. Liu, C. Nuckolls, *Adv. Mater.* 2010, **22**, 3282

16 H. Zhang, X. Guo, J. Hui, S. Hu, W. Xu, D. Zhu, *Nano Lett.* 2011, **11**, 4939; C.-W. Tseng, D.-C. Huang, Y.-T. Tao, *ACS Appl. Mater. Interfaces* 2012, **4**, 5483; M. Yoshida, K. Suemori, S. Uemura, S. Hoshino, N. Takada, T. Kodzasa, T. Kamata, *Jpn. J. Appl. Phys*. 2010, 49.

17 L. A. Frolova, P. A. Troshin, D. K. Susarova, A. V. Kulikov, N. A. Sanina, S. M. Aldoshin. *Chem. Comm*., 2015, **51**, 6130.

Graphical abstract

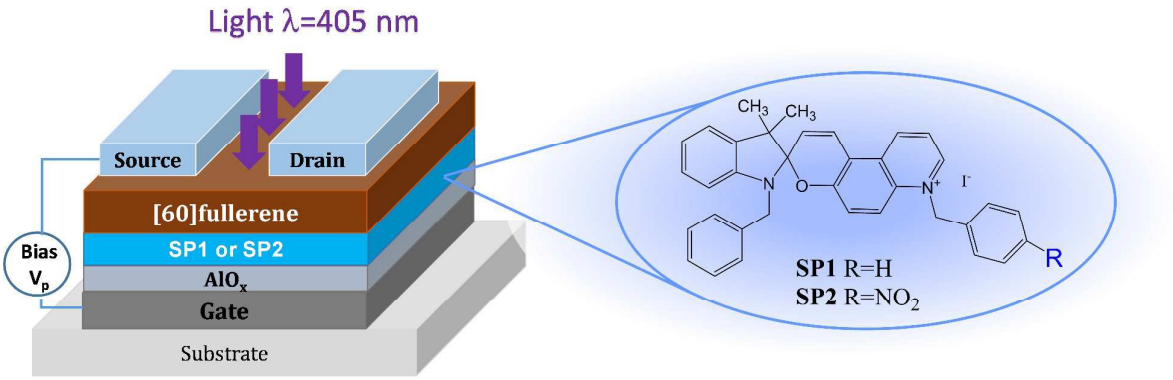

Optical memory devices based in photoswitchable OFETs comprising light sensitive layers of photochromic spiropyran salts revealed advanced electrical characteristics and superior stability